Article

Oligoarginine-Conjugated Peptide Foldamers Inhibiting Vitamin D Receptor-Mediated Transcription

Mami Takyo, Yumi Sato, Naoya Hirata, Keisuke Tsuchiya, Hiroaki Ishida, Takashi Kurohara, Yuta Yanase, Takahito Ito, Yasunari Kanda, Keiko Yamamoto, Takashi Misawa,* and Yosuke Demizu*

Read Online

ACCESS | Metrics & More | Article Recommendations | Supporting Information

ABSTRACT: The vitamin D receptor (VDR) is a nuclear receptor, which is involved in several physiological processes, including differentiation and bone homeostasis. The VDR is a promising target for the development of drugs against cancer and bone-related diseases. To date, several VDR antagonists, which bind to the ligand binding domain of the VDR and compete with the endogenous agonist $1\alpha,25(OH)D_3$, have been reported. However, these ligands contain a secosteroidal skeleton, which is chemically unstable and complicated to synthesize. A few VDR antagonists with a nonsecosteroidal skeleton have been reported. Alternative inhibitors against VDR transactivation that act via different mechanisms are desirable. Here, we developed peptide-based VDR inhibitors capable of disrupting the VDR−coactivator interaction. It was reported that helical SRC2-3 peptides strongly bound to the VDR and competed with the coactivator in vitro. Therefore, we designed and synthesized a series of SRC2-3 derivatives by the introduction of nonproteinogenic amino acids, such as β-amino acids, and by side-chain stapling to stabilize helical structures and provide resistance against digestive enzymes. In addition, conjugation with a cell-penetrating peptide increased the cell membrane permeability and was a promising strategy for intracellular VDR inhibition. The nona-arginine-conjugated peptides **24** with side-chain stapling and **25** with cyclic β-amino acids showed strong intracellular VDR inhibitory activity, resulting in suppression of the target gene expression and inhibition of the cell differentiation of HL-60 cells. Herein, the peptide design, structure−activity relationship (SAR) study, and biological evaluation of the peptides are described.
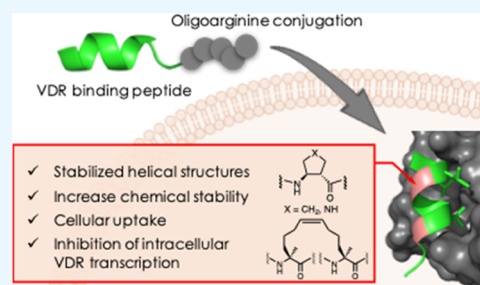
INTRODUCTION

The vitamin D receptor (VDR), a member of the family of nuclear receptors, regulates the transcriptional activation of target genes and is involved in diverse physiological functions, including calcium homeostasis and cell differentiation.[1] Overactivation of the VDR has been known to contribute to the development of Paget's disease of bone,[2] a rare disease; therefore, VDR inhibitors have attracted attention as therapeutic agents for Paget's disease. VDR antagonists that bind to the ligand binding domain (LBD) of the VDR and compete with the endogenous agonist $1\alpha,25(OH)_2D_3$ have been reported (Figure S1).[3−9] However, these ligands contain a secosteroidal skeleton, which is chemically unstable and complicated to synthesize. Some VDR antagonists with a nonsecosteroidal skeleton have been reported.[10] The development of inhibitors against VDR transactivation via different mechanisms is desirable. In this study, we focused on the VDR−coactivator interaction, which is important for VDR transcriptional activation. The binding of calcitriol [VD₃: $1\alpha,25(OH)_2D_3$], an endogenous agonist, to the VDR induces a conformational change that allows the VDR to interact with coactivators, leading to transcriptional activation. It has been reported that the coactivator binds to the VDR via a helical structure containing a conserved LXXLL sequence (L: leucine,

X: any amino acid).[11,12] Ishikawa et al. reported that small molecules that mimic the LXXLL motif showed inhibition of VDR transcriptional activity with a half maximal inhibitory concentration (IC_{50}) value of 14 μM.[13] Their results suggested that molecules that inhibit the interaction between the VDR and the coactivator could be promising candidates for VDR inhibitors. Yamamoto and co-workers reported that the SRC2-3 peptide was bound to the VDR with high affinity, and X-ray crystal structural analysis demonstrated that SRC2-3 was bound to the VDR via a helical structure.[14] Guichard et al. reported that oligourea-based foldamers based on SRC2-3 formed a helical structure, showed a high affinity to the VDR, and inhibited the VDR−coactivator interaction.[15] In general, oligopeptides are useful in the development of protein−protein interaction (PPI) inhibitors because their large molecular weight allows the oligopeptides to bind to a wide range of binding interfaces.[16] However, the low proteolytic stability and
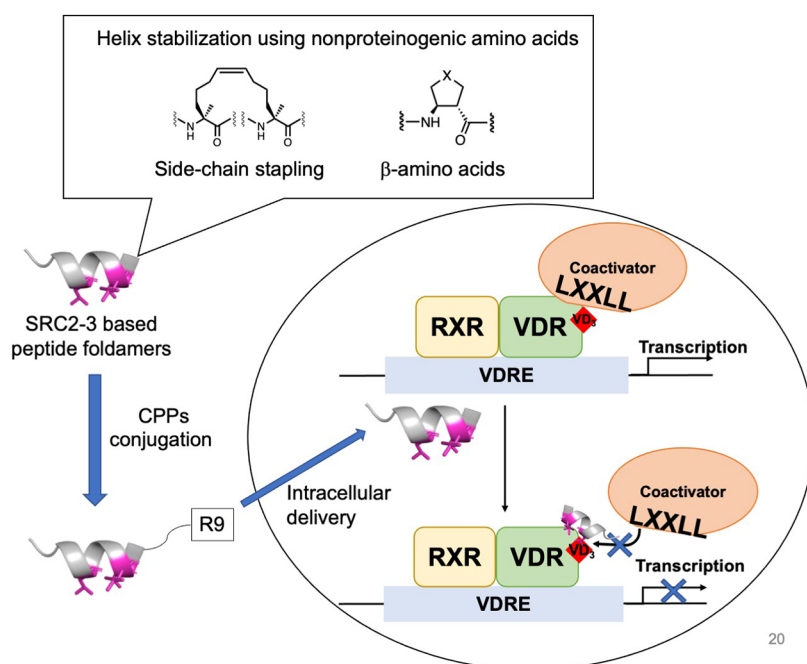
Figure 1. Development of helix-stabilized SRC2-3 derivatives using nonproteinogenic amino acids for the inhibition of intracellular VDR-mediated transcription.

the lack of the cell membrane permeability of oligopeptides are problematic for the development of PPI inhibitors targeting intracellular proteins.[17,18] The formation of the appropriate secondary structures of peptide drugs is required to exert the desired biological functions. However, short peptides are not able to form stable secondary structures and therefore cannot exert such biological functions. In addition, short peptides are easily degraded by enzymes in vivo, making it difficult to develop intracellular PPI inhibitors based on peptides.[18,19] For this reason, there are no examples of PPI inhibitors targeting the VDR−coactivator interaction in cells. In recent years, to overcome the abovementioned problems, nonproteinogenic amino acids (AAs) have been introduced into peptide sequences, which can stabilize the secondary structure and impart in vivo stability.[20−23] Oligomers that form such stable secondary structures are called foldamers[24] and are expected to be useful in material and medicinal chemistry.[25] To date, most foldamers contain building blocks such as β-amino acids (β-AAs)[17] or quinolone moieties[21] or have side-chain stapling.[22] In our laboratory, we have previously reported that the introduction of α,α-disubstituted amino acids into short peptides can stabilize the helical structure and improve the bioactivity.[23,26] We have also developed inhibitors of the VDR−coactivator interaction by the introduction of side-chain stapling into a sequence containing the LXXLL motif.[27] Here, we investigated the effects of the introduction of non-proteinogenic amino acids, such as β-amino acids, and side-chain stapling into the SRC2-3 sequence on the stabilization of the helical structure and the binding affinity with the VDR. Generally, oligopeptides have poor cell membrane permeability and cannot exert biological actions in cells.[18] To overcome this problem, cell-penetrating peptides (CPPs) have been used to improve the cell membrane permeability of oligopeptides. Previously, we have developed intracellular estrogen receptor (ER) inhibitors based on the PERM-3 peptide that inhibited the interaction between the ERs and coactivators.[28] This research indicated that the conjugation of an oligoarginine, as a

CPP, with PERM-3 dramatically enhanced the intracellular delivery of PERM-3 and enabled the inhibition of ER-mediated transcription. Using these results, we designed and synthesized oligoarginine-conjugated SRC2-3 derivatives and investigated the effect of the derivatives on the intracellular delivery of peptides and the inhibition of intracellular VDR transcription (Figure 1).

RESULTS AND DISCUSSION

Peptide Design and Synthesis. To investigate the effect of the introduction of nonproteinogenic AAs on the secondary structure and biological functions of SRC2-3, we designed and synthesized a series of SRC2-3 derivatives, **1−25**, as shown in Table 1. Peptides **1−5** possess side-chain hydrocarbon stapling between the i and $i + 4$ positions to avoid substitution of Leu residues in the LXXLL motif. α/β-Peptides **6−18** have acyclic or cyclic β-amino acid (β-AA) residues introduced into the SRC2-3 sequence. Gellman and co-workers revealed that the introduction of β-amino acid residues to peptides in a specific manner, such as $\alpha\alpha\beta$, $\alpha\alpha\alpha\beta$, or $\alpha\alpha\beta\alpha\alpha\alpha\beta$, can provide peptides capable of adopting an α-helix-like conformation.[29] Moreover, the replacement of hydrophobic and cationic residues with cyclic β-AAs, (3R,4S)-trans-2-aminocyclopentane carboxylic acid (ACPC) and (3R,4S)-trans-4-aminopyrroli-dine-3-carboxylic acid (APC), can stabilize helical structures without any polarity change. We designed and synthesized CPP-conjugated SRC2-3 derivatives to improve cell membrane permeability. Oligoarginine is a representative CPP and induces intracellular uptake via endocytosis.[30,31] Therefore, oligoarginine peptides with different lengths (peptides **19**, **20**, and **21**: n = 3, 6, and 9, respectively) were attached to the C-terminus of SRC2-3. In addition, N-terminal R9-conjugated peptide **22** and C-terminal R9-conjugated peptides **23−25** were prepared. All peptides were synthesized by Fmoc solid-phase synthesis and purified using reverse-phase high-perform-ance liquid chromatography (HPLC).

Table 1. Sequences of SRC2-3 Derivatives[a]

Peptide	Sequence
SRC2-3	K E N A L L R Y L L D K D
1	S₅* E N A S₅* L R Y L L D K D
2	K E S₅* A L L S₅* Y L L D K D
3	K E N S₅* L L R S₅* L L D K D
4	K E N A L L S₅* Y L L S₅* K D
5	K E N A L L R S₅* L L D S₅* D
6	K E N A L L R Y L L D K D
7	K E N X L L R Y L L D K D
8	Z E N A L L R Y L L D K D
9	K E N A L L R Y L L D K D
10	K E N A L L R Y L L D K D
11	K E N X L L R Y L L D K D
12	K E N A L L Z Y L L D K D
13	K E N A L L R Y L L D K D
14	K E N X L L R Y L L D K D
15	K E N A L L R Y L L D Z D
16	K E N A L L R Z L L D K D
17	K E N X L L R Y L L D Z D
18	K E N X L L R Z L L D Z D
19	K E N A L L R Y L L D K D (G)₃(R)₃
20	K E N A L L R Y L L D K D (G)₃(R)₆
21	K E N A L L R Y L L D K D (G)₃(R)₉
22	(R)₉(G)₃ K E N A L L R Y L L D K D
23	K E N S₅* L L R S₅* L L D K D (G)₃(R)₉
24	K E N A L L R S₅* L L D S₅* D (G)₃(R)₉
25	K E N X L L R Y L L D Z D (G)₃(R)₉

S₅*, S₅*: Side chain stapling

● : β-AA
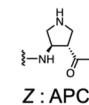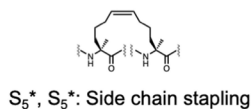
X : ACPC

Z : APC

[a]The β-AA residues are indicated by blue circles. The non-proteinogenic amino acids are indicated in red. The N-termini and C-termini of all of the peptides were in free and amide forms, respectively. S₅: (S)-pentenyl alanine; X: ACPC; Z: APC. The chemical structures of the nonproteinogenic amino acids are shown. The cyclization between i and $i + 4$ of two S₅ residues is indicated by an asterisk.

Secondary Structure Analysis. To examine the preferred secondary structure of the synthesized peptides, the circular dichroism (CD) spectra of **1−25** were measured in pH 7.4 phosphate buffer solution (PBS, Figures 2 and S2). In the spectra, stapled peptides **3−5** showed negative maxima at approximately 208 and 222 nm, indicating the formation of an α-helical structure. Stapled peptides **1** and **2** did not form an α-helical structure. These results suggested that the C-terminal stapling of SRC2-3 may be more favorable for stabilizing the helical structure compared with N-terminal stapling.

Peptides **6−10** and **13**, which have three or four acyclic β-AAs, did not form α-helical structures. In addition, peptides **11** and **12** also did not form an α-helical structure, indicating that the ααβαααβ pattern is not adequate for the formation of an α-helical structure in SRC2-3. In contrast, peptide **14** with two acyclic β-AAs and one ACPC in an αααβ pattern showed negative maxima at 204 nm,[32] indicating that peptide **14** formed an α-helix-like structure; however, peptides **15** and **16** did not form helical structures. These data indicated that the replacement of the 4th Ala residue with ACPC tended to stabilize the helical structure, and the additional introduction of cyclic β-AAs in an αααβ pattern also stabilized α-helix-like structures. Peptides **17** and **18** bearing two or three cyclic β-AA residues formed more stable α-helix-like structures compared with peptides bearing only one cyclic β-AA. We also investigated the effect of R9 conjugation on the preferred secondary structures. Peptides **23−25** with side-chain stapling or β-amino acids formed helical structures, while peptide **21** did not form a helical structure. The stabilization of the helical structures by introducing side-chain stapling or β-amino acids was maintained even after R9 conjugation (Figure S3).

Inhibition of the VDR−Coactivator Interaction Measured by a Fluorescein Polarization (FP) Assay. We investigated the inhibitory activity of the synthesized peptides **1−18** toward the VDR−coactivator interaction using a competitive FP assay. Recombinant VDR proteins were prepared according to a previously reported method.[33] Briefly, pET28a/rVDRD, which is the ligand binding domain of rat VDR with a deleted loop region (Ser165−Pro211), was
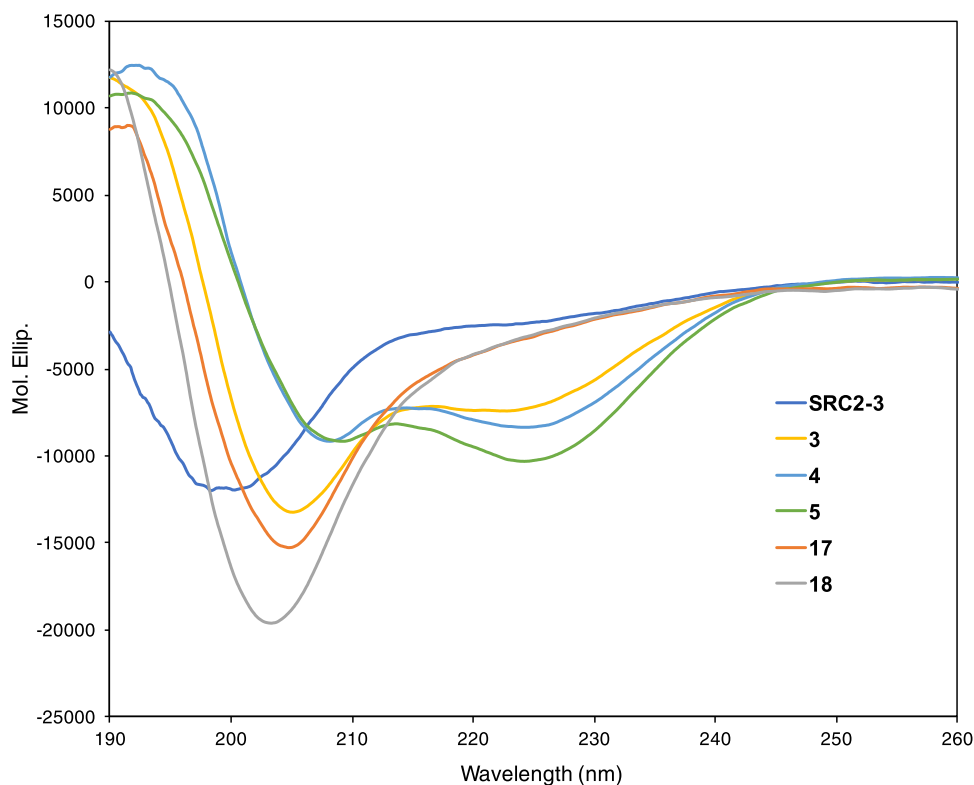

Figure 2. Preferred secondary structures of SRC2-3 and the synthesized peptides **3−5** and **17−18** in pH 7.4 PBS. Peptide concn: 200 μM.

transformed into KRX competent cells and incubated with rhamnose for 16 h at 25 °C. The lysis solution containing the VDR proteins was purified using a HisTrap column and concentrated. The competitive FP assay was conducted using fluorescein-conjugated SRC2-3, and the competitive activity was evaluated by cotreatment with the tested peptides. The inhibitory activity of the peptides is presented as the relative IC_{50} value compared with SRC2-3. As shown in Table 2, α-

Table 2. Inhibition of the VDR−Coactivator Interaction by Synthesized Peptides 1−18 Using FP Assays[a]

peptide	relative value of IC_{50}	peptide	relative value of IC_{50}
SRC2-3	1.00 (3.37 ± 1.15)	**10**	1.64 ± 0.55
1	>254	**11**	2.52 ± 0.14
2	>254	**12**	2.11 ± 0.58
3	1.95 ± 0.50	**13**	1.81 ± 0.49
4	3.37 ± 0.31	**14**	1.84 ± 0.58
5	2.26 ± 0.30	**15**	0.89 ± 0.14
6	1.01 ± 0.06	**16**	1.88 ± 0.43
7	1.90 ± 0.12	**17**	1.20 ± 0.26
8	1.12 ± 0.23	**18**	2.53 ± 0.14
9	1.99 ± 0.46		

[a]The inhibitory activities of peptides SRC2-3 and **1−18** on the VDR−coactivator interaction are shown as the IC_{50} values relative to that of SRC2-3. Data are expressed as the means ± standard error (SE) of three independent experiments. FAM-SRC2-3 concn: 10 nM.

helical peptides **3−5** showed comparable inhibitory activity with SRC2-3, while peptides **1** and **2**, which were random structures, exhibited weak inhibitory activity, suggesting that the introduction of side-chain stapling on the opposite side of the VDR binding interface tended to increase the inhibitory activity of the peptides. Peptides **6−18**, containing β-amino acids, showed moderate inhibitory activity, comparable with SRC2-3. Among them, peptides **8**, **15**, and **17** showed higher inhibitory activity compared with the other tested peptides, indicating that the replacement of a Lys residue with an APC residue increased the inhibitory activity by maintaining the polarity while stabilizing the α-helical structure. Moreover, we confirmed that the conjugation of R9 to SRC2-3 and **5** did not affect their binding activity, as shown in Figure S4.

Chemical Stability Analysis of the Peptides. The effect of the introduction of stapling and β-AAs into the SRC2-3 sequence on the chemical stability toward a digestive enzyme was investigated. Peptides **3**, **5**, and **17**, which formed helical structures and also showed relatively good inhibitory activity, were used to evaluate the susceptibility to proteolysis with proteinase K, which is a serine proteinase that cleaves the C-terminus of hydrophobic AAs. As expected, SRC2-3, composed of only proteinogenic AAs, was rapidly degraded under experimental conditions (half-life: $t_{1/2}$ = 3.0 h), and liquid chromatography−mass spectrometry (LC−MS) analysis revealed three major cleavage sites, as shown in Figure S5. The half-life of peptides **3**, **5**, and **17**, was prolonged compared with SRC2-3 ($t_{1/2}$; **3**: > 72 h, **5**: 41 h, **17**: 19 h), indicating that the introduction of nonproteinogenic AAs endowed resistance against this digestive enzyme.

Intracellular VDR Inhibition Using a Reporter Gene Assay. The ability of the peptides to inhibit VDR-mediated transcription in the presence of $1\alpha,25(OH)_2D_3$ (30 nM) was assessed using a reporter gene assay using MCF-7 cells expressing the VDR. To improve the membrane permeability

of the peptides, oligoarginines (R_n; **19**: n = 3, **20**: n = 6, and **21**: n = 9) were introduced into the C-terminus of SRC2-3 (peptides **19−21**). In addition, peptide **22** with an N-terminal R_9 sequence was synthesized to investigate whether the position of the oligoarginine affected the inhibitory activity. The inhibitory activity of the peptides is presented as the value relative to the inhibitory activity of SRC2-3. Peptides **19** and **20**, which have three (R_3) or six arginine (R_6) residues, showed no or weak inhibitory activity, but peptides **21** and **22** showed potent inhibitory activity against VDR transactivation. These data indicated that the introduction of nona-arginine (R_9) into the SRC2-3 sequence was required for intracellular delivery, but the position of the nona-arginine did not affect the inhibitory activity. Peptides **3**, **5**, and **17**, which formed α-helical structures and also had relatively strong inhibitory activity toward the VDR−coactivator interaction, were conjugated with R_9, and the VDR inhibitory activity was investigated. In the reporter gene assay, peptides **24** and **25** had slightly stronger activity compared with peptide **21** (IC_{50} values of 0.77 and 1.16 μM for **24** and **25**, respectively); 3 μM peptide **23** showed 44.3% inhibition, but peptide **23** showed the cytotoxicity against MCF-7 cells at 10 μM. Therefore, the IC_{50} value of **23** could not be calculated. Peptide **3**, which is the core peptide of peptide **23**, showed strong inhibition of the VDR−coactivator interaction, but the inhibition of the VDR transactivation was weak. On the other hand, the LXXLL sequence is highly conserved in the nuclear receptor family, hence the synthesized peptides might inhibit these families. Therefore, the intracellular estrogen receptor (ER)-mediated transcription assay was performed, as shown in Figure S6. As a result, peptides **21**, **24**, and **25** showed the inhibitory activity of ER-mediated transcription. It is demonstrated that peptides **21**, **24**, and **25** were not specific for VDR. Next, we investigated the mechanism of action of the peptides to investigate how the peptides exerted VDR inhibitory activity in cells. The intracellular uptake was investigated using flow cytometry and confocal microscopy observations (Figures S7 and S8). The flow cytometry analysis indicated that peptides **3**, **5**, and **16** did not internalize into cells, while peptides **21**, **23**, **24**, and **25** were quantitatively internalized into the cells. These data suggested that conjugation with a CPP fragment was essential for the efficient delivery of the peptides. Moreover, confocal microscopy observation analysis indicated that peptides **24** and **25** were broadly localized over the entire cell, while treatment with peptide **23** resulted in a bright point, indicating that peptide **23** was localized in the endosome. From these data, we presumed that peptide **23** was trapped in the endosome and could not exert inhibitory activity. The cytotoxicity of the peptides against MCF-7 cells was also evaluated (Figure S9). R_9-unconjugated peptides SRC2-3, **3**, **5**, and **16** did not show any cytotoxicity up to 100 μM, whereas R_9-conjugated peptides **21**, **23**, **24**, and **25** had strong cytotoxicity at 10 μM. It has been reported that amphipathic helical peptides such as antimicrobial peptides disrupt the cell membrane and induce cytotoxicity against human cells.[34] The introduction of nonproteinogenic amino acid increased the and R9 conjugation increased the amphipathicity of the peptides, hence the cytotoxicity of the R9-conjugated peptides was induced at high concentrations (Table 3).

Quantitative Polymerase Chain Reaction (PCR) Analysis of p21 mRNA for VDR-Mediated Transcription. The transcriptional inhibition of downstream genes by R_9-conjugated peptides **21**, **24**, and **25** was evaluated. It has been

**Table 3. Inhibition of VDR-Mediated Transcriptional Activity by Treatment with Synthesized Peptides 19−25[a]**

peptide	IC50 (μM)
SRC2-3	>100
19	>30
20	>30
21	2.17 ± 0.62
22	2.03 ± 0.29
23	44.3%[b]
24	0.77 ± 0.35
25	1.16 ± 0.50

[a]The activation rate by treatment of 30 nM calcitriol was defined as 100%. Data are expressed as the means ± SE of three independent experiments. [b]% Inhibition at 3 μM.

reported that the expression of the cyclin-dependent kinase p21 gene is upregulated via VDR-mediated transcription by treatment with VD$_3$.[35] Transcriptional analysis of p21 was performed using HL-60 cells that had been incubated for 24 h in the presence of $1\alpha,25(OH)_2D_3$ (30 nM) with or without the peptides. The resulting mRNA was extracted from the lysate and PCR analysis was performed to investigate the VDR-mediated transcriptional activity (Figure 3). The relative p21 mRNA expression levels were decreased by treatment with 10 μM peptides, while treatment with 1 μM peptides did not affect the p21 gene levels. The expression level of the p21 gene was positively correlated with the VDR transcriptional inhibitory activity measured by the reporter gene assay, indicating that peptides **21**, **24**, and **25** were internalized into even nonadherent cells (HL-60 cells) and inhibited the VDR transactivation and suppressed the target gene transcription.

Inhibitory Activity of VDR-Mediated Cell Differentiation. It has been reported that $1\alpha,25(OH)_2D_3$ can induce the cell differentiation of HL-60 cells via VDR transcriptional activity. Therefore, we evaluated whether the peptides inhibited HL-60 cell differentiation using a nitroblue tetrazolium (NBT) reduction assay (Figure 4). Briefly, HL-60 cells were incubated with 30 nM VD$_3$ with or without peptides, the cells were treated with NBT solution, and the reduction in NBT activity was detected as HL-60 differentiation. Treatment with 1 μM peptides **21**, **24**, or **25** did not inhibit cell differentiation, but at 10 μM, peptides **24** and **25** effectively inhibited cell differentiation compared with peptide **21**. This result may be because the introduction of nonproteinogenic amino acids improved the stability of the peptides in the cells, allowing the peptides to function for a long time.

Docking Simulation of Peptides with the VDR-LBD. The analysis of the binding of the peptides with the VDR by docking studies was performed by Molecular Operating Environment (MOE) using the X-ray cocrystal structure of the peptides bound to the LXXLL motif obtained from the Protein Data Bank (PDB: 5H1E).[14] As shown in Figures 5 and S10, the three Leu residues (colored red) of peptides **5** and **17** were oriented to the binding surface of the VDR in the same manner as for SRC2-3. The Leu residues at positions 6 and 9 of peptides **5** and **17** interacted with the hydrophobic residues Ile256 and Leu259 of the VDR-ligand binding domain (LBD), while the Leu residue at position 8 interacted with Ile238 of the VDR-LBD. The binding modes of each peptide, SRC2-3, **5**, and **17**, and the essential amino acid residues involved in the interaction are shown in Figure S10. The docking studies indicated that peptides **5** and **17** mimicked the LXXLL sequence of SRC2-3, and the three Leu residues played an important role in the interaction. Peptide **5** showed a different binding mode compared with that of SRC2-3 and **17**. This
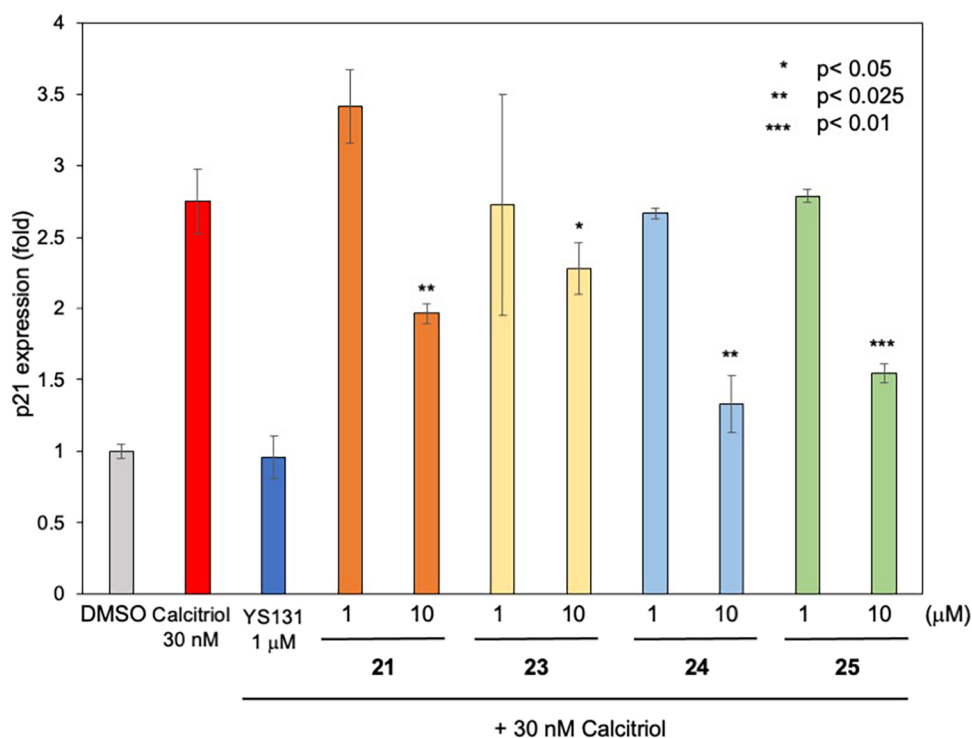
Figure 3. Suppression of p21 mRNA levels by treatment with peptides **21** and **23−25**. YS131 is a reported secosteroidal antagonist[7] for VDR and was used as a positive control. Data in the bar graphs are means ± standard deviation (SD, error bars) of three independent experiments.
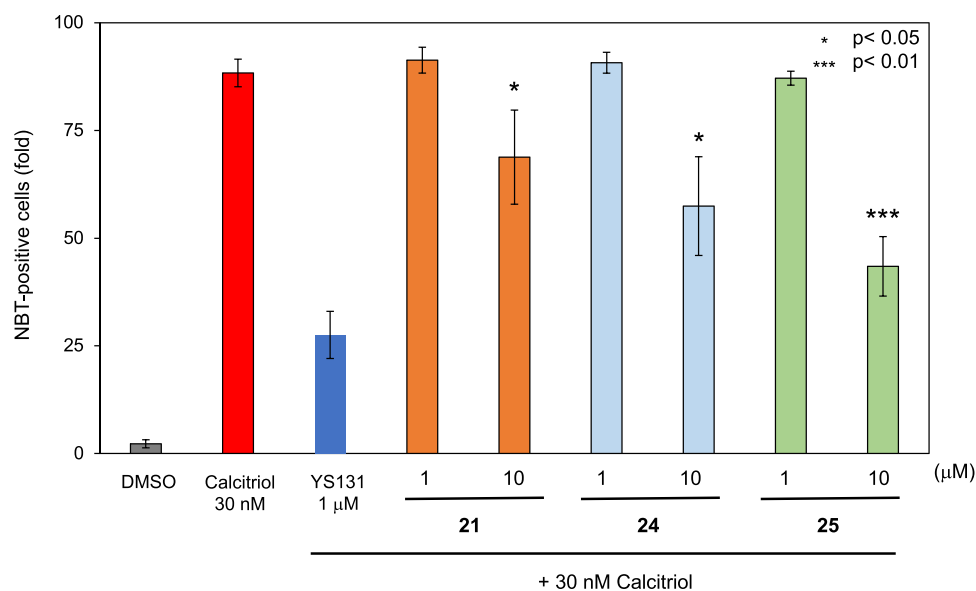
Figure 4. Inhibition of HL-60 cell differentiation by peptides **21**, **24**, and **25** at the indicated concentrations. Data in the bar graphs are means ± SD (error bars) of three independent experiments.
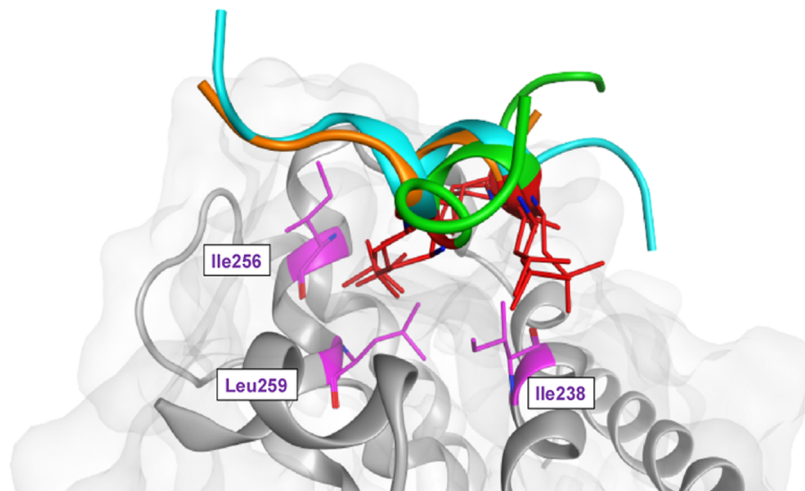
Figure 5. Potential interactions of peptides SRC2-3 (crystal structure; 5H1E [14]), **5**, and **17** binding to the LBD of the VDR (PDB:5H1E).[14] The binding structures of peptides **5** and **17** were calculated with MOE 2020.09. SRC2-3, **5**, and **17** are colored orange, green, and cyan, respectively. The amino acids of the VDR related to the interaction are shown in purple.

difference is presumably because of the introduction of side-chain stapling, which stiffens the main chain of the peptide and creates a different structure compared with the linear peptides.

In this study, we designed and synthesized a series of SRC2-3 derivatives by the introduction of nonproteinogenic AAs, such as β-AAs, and by side-chain stapling. CD spectra analysis revealed that the introduction of side-chain stapling or multiple cyclic β-AAs stabilized the helical structures of the peptides, while the introduction of three or four acyclic β-AAs tended to destabilize the secondary structures. FP assays were conducted to investigate the ability of the synthesized peptides to disrupt the VDR−coactivator interaction. Peptides **1** and **2**, which did not form stable secondary structures, showed weak inhibition of the VDR−coactivator interaction, while peptides **3**−**5**, which formed α-helical structures, had moderate inhibitory activity. These experiments indicated that the formation of a stabilized helical structure improved the inhibitory activity of the peptides. Peptides **6**, **8**, **15**, and **17**, which contain multiple

β-AAs, showed strong binding to the VDR, although peptides **6**, **8**, and **15** did not form a stable helical structure as indicated by the CD spectra. On the other hand, it has been reported that the formation of a rigid structure could prevent the induced fit to the target proteins and decrease their binding affinities.[36] Therefore, peptides **6**, **8**, and **15** did not form stable helical structures, which might show potent binding activity against VDR via the induced fit. To develop intracellular VDR inhibitors, CPP-conjugated peptides **19**−**25** were designed. A reporter gene assay indicated that the conjugation of a nona-arginine sequence was required for effective intracellular uptake and VDR inhibition. Peptide **20**, which is the R$_9$-conjugated derivative of peptide **3**, showed weak inhibition of intracellular VDR transcription, although peptide **3** showed moderate inhibition of the VDR−coactivator interaction. The intracellular estrogen receptor (ER)-mediated transcription assay was also performed to investigate the specificity of the peptides on VDR (Figure S6). As a result, peptides **21**, **24**, and

25 showed the inhibitory activity of ER-mediated transcription. It is demonstrated that peptides **21**, **24**, and **25** were not specific for VDR and could inhibit other nuclear receptors. The further structural development for selective inhibition of intracellular VDR-mediated transcription was under investigation. Mechanistic analysis using confocal microscopy observations indicated that the appropriate delivery of peptides to the intracellular cytosol was essential for disrupting the intracellular VDR−coactivator interaction. Peptides **24** and **25** inhibited VDR-mediated target gene transcription, and the inhibition of p21 transcription was positively correlated with the inhibitory activity in the reporter gene assay. Moreover, peptides **24** and **25** could be internalized into even nonadherent cells and inhibited the VDR-mediated differentiation in HL-60 cells. Our peptide design strategy, using the introduction of nonproteinogenic AAs and the conjugation of CPP fragments, could provide peptides with stabilized helical structures and increased chemical stability against digestive enzymes. Therefore, the effective delivery to the cytosol and the long-lasting effect of the peptides on the disruption of the intracellular VDR−coactivator interaction were enabled. Peptides **24** and **25** may be promising candidates for therapeutic agents to treat Paget's disease of bone.

CONCLUSIONS

A series of SRC2-3 derivatives with different secondary structures were developed in this study. The introduction of nonproteinogenic AAs, such as β-AAs, and side-chain stapling in the SRC2-3 sequence could stabilize the α-helical structure and thereby increase the binding affinity toward the VDR. Peptides **24** and **25** were able to be delivered into cells by conjugation with CPPs and inhibited the VDR-mediated transcriptional activity in the cells. Peptide **25** also suppressed the target gene expression by the inhibition of VDR-mediated transcriptional activity, resulting in the inhibition of the VDR-mediated cell differentiation of HL-60 cells. The structural control of peptides and peptide conjugation with CPPs are useful tools in the design of inhibitors of intracellular PPIs and are expected to be used in the future development of inhibitors targeting intracellular transcriptional factors.

EXPERIMENTAL SECTION

Synthesis and Characterization of Peptides. Peptides **1**−**18** were synthesized using microwave-assisted Fmoc-based solid-phase methods on a Rink Amide ProTide Resin (LL, CEM) by a Liberty Blue Automated Microwave Peptide Synthesizer (CEM). The following describes a representative coupling and deprotection cycle at a 50 μmol scale. The Rink Amide ProTide Resin (LL) was soaked for 10 min in CH_2Cl_2. After that, Fmoc-amino acid (4 equiv), Oxyma Pure (4 equiv), and N,N'-diisopropylcarbodiimide (DIC, 10 equiv) dissolved in a solution of dimethylformamide (DMF) were added to the resin. Deprotection of Fmoc protective groups was carried out using 20% piperidine in DMF.

Peptides **19**−**25** were synthesized using Fmoc-based solid-phase methods on a NovaPEG Rink amide resin by a SyroI (Biotage). The following describes a representative coupling and deprotection cycle at a 50 μmol scale. The NovaPEG Rink amide resin was soaked for 30 min in CH_2Cl_2. After that, Fmoc-amino acid (4 equiv), HBTU (6 equiv), HOBt (6 equiv), and N,N-diisopropylethylamine (DIPEA, 10 equiv) dissolved in a solution of DMF were added to the resin.

Deprotection of Fmoc protective groups was carried out using 20% piperidine in DMF.

Ring closing metathesis reactions were performed using a 20 mol % 2nd generation Grubbs catalyst in 1,2-dichloroethane. After the peptide synthesis, the resin was suspended in a cleavage cocktail (95% TFA, 2.5% water, 2.5% triisopropylsilane) for 2 h at room temperature. The TFA solution was evaporated to a small volume under a stream of N_2 and dripped into cold ether to precipitate the peptides. The crude peptides were dissolved in dimethylsulfoxide (DMSO) and purified by reversed-phase HPLC using an Inertsil WP300 C18 (5 μm, 20 × 250 mm). After purification, the peptide solutions were lyophilized. Peptide purity was assessed using analytical HPLC and an Inertsil WP300 C18 (5 μm, 4.6 × 250 mm), and the peptides were characterized by LCMS-ion trap-time-of-flight (LCMS-IT-TOF, Shimadzu).

CD Spectra. Peptides were dissolved in 20 mM phosphate buffer (pH 7.4) at a concentration of 200 μM. CD spectra were measured with a CD spectrometer J-1100 (JASCO) using the following parameters: wavelength: 190−260 nm, bandwidth: 1 nm, response: 1 s, speed: 50 nm/min, accumulations: three times, and path length: 1 nm.

Enzyme Resistance of Peptides. In total, 50 μL of 1 mM peptide solution, 1 μL of proteinase K (Takara Bio) 0.0005% solution in phosphate buffer (pH 7.4), and 49 μM of phosphate buffer (pH 7.4) were added to the microtubes and incubated at 37 °C for each time. After each incubation, the reaction was stopped by adding 100 μL of water/acetonitrile (1/1) solution. The samples were assessed by using analytical HPLC and an Inertsil WP300 C18 (5 μm, 4.6 × 250 mm), and the area ratio was calculated.

The enzymatic cleavage sites were identified by LCMS-ion trap-time-of-flight (LCMS-IT-TOF, Shimadzu).

Protein Expression and Purification. The pET28a/rVDRD plasmid, provided by N. Ito, was expressed in KRX (Promega) grown at LB with 50 μg/mL kanamycin. VDR-LBD protein expression was induced with 0.1% rhamnose for 16 h at 25 °C, and the KRXs were lysed with lysis buffer. Proteins were purified by a HisTrap Column (Capturem His-Tagged Purification Large Volume, Takara Bio USA, Inc.).

Fluorescein Polarization Assay. The fluorescein polarization-based binding assay for fluorescein-labeled SRC2-3 was performed using VDR-LBD. In brief, test compounds were serially diluted from 254 to 0.015 μM in assay buffer (50 mM sodium phosphate, 150 mM NaCl, 1 mM dithiothreitol, 1 mM ethylenediaminetetraacetic acid (EDTA), 0.01% NP-40, 10% glycerol, pH 7.2) in nonbinding black 384-well plates. Then, 10 μL of VDR-LBD, $1\alpha,25(OH)_2D_3$, and fluorescein-labeled SRC2-3 mixed solution was added, yielding each final concentration of 5 μM, 5 μM, and 10 nM, respectively. The samples were allowed to equilibrate for 3 h at room temperature. The plates were then measured using fluorescein polarization (excitation wavelength: 470 nm, emission wavelength: 530 nm) on an EnVision Multilabel Plate Reader (PerkinElmer, Waltham, MA). The measurements of fluorescence polarization of a molecule (mP) are performed in the fluorescence polarization mode. The percentage of inhibition of test compounds was calculated according to the following equation where mPsample is the value of the wells containing test compounds and mP100% is the value of the maximum binding well. The concentration of test compounds that reduces the mP value by 50% (IC_{50}) was estimated from a

graph plotting the mP value versus the concentration of the compounds on the semi-log axis.

percentage of inhibition

$$= [(mP100\% - mPsample)/mP100\%] \times 100$$

TR-FRET Assay. The TR-FRET assay for R9-unconjugated and -conjugated peptides was performed using a Lanthascreen TR-FRET VDR coactivator assay kit (Thermo Fischer). Briefly, test peptides were serially diluted from 20000 to 0.256 μM in assay buffer in nonbinding black 384-well plates. Then, 5 μL of VDR-LBD, calcitriol, and fluorescein-labeled TRAP220/DRIP-2P/Tb anti-GST antibody mixed solution was added, yielding each final concentration of 1, 3, and 400 nM, respectively. The samples were allowed to equilibrate for 2 h at room temperature. TR-FRET was measured on an EnVision Multilabel Plate Reader (PerkinElmer, Waltham, MA) using a 520 nm fluorescein emission filter and a 490 nm terbium emission filter.

Cell Culture. MCF-7 cells and HL-60 cells were cultured in a Roswell Park Memorial Institute-1640 (RPMI-1640) medium (Sigma-Aldrich, St. Louis, MO) containing 10% heat-inactivated fetal bovine serum (FBS, Thermo Fisher Scientific, Waltham, MA) and 1% penicillin/streptomycin. MCF-7 cells were purchased from ATCC (Manassas, VA).

Dual-Luciferase Reporter Gene Assay. MCF-7 cells were seeded onto 24-well plates at a density of 4×10^4 cells/well and cultured for 24 h. Then, the cells were transfected with the firefly luciferase reporter plasmid containing VDRE and Renilla luciferase plasmid-SV40 as control by Lipofectamine LTX Invitrogen. After 8 h, the cells were treated with the indicated concentrations of each test compound. After 16 h incubation, the luciferase activities of the cell lysates were measured by a Dual-Luciferase Reporter Assay System (Promega). The ER-mediated transcription assay was performed as the same procedure using the reporter plasmid containing estrogen receptor-responsible elements (EREs).

Flow Cytometry. MCF-7 cells were seeded onto 6-well plates at a density of 4×10^4 cells/well and cultured for 24 h. Then, the cells were incubated with the peptide for 2 h. After incubation, the plates were washed with PBS supplemented with heparin (20 units/mL) and PBS and detached by the treatment of trypsin-EDTA. The collected cells were pelleted by centrifugation at 1500 rpm for 5 min, and the supernatant was removed. After washing with PBS, the collected cells were suspended in 500 μL of PBS, and the mean fluorescence intensity in cells was measured by a flow cytometer (BD Accuri C6 Plus Flow Cytometer).

Confocal Microscope Observation. MCF-7 cells were plated onto 35 mm grass-bottom dishes (MATSUNAMI). The cells were incubated with peptide (1 μM) and LysoTracker (70 nM) for 2 h and then incubated with Hoechst33342 (0.5 μL/well) for 5 min. After washing with PBS, fluorescent images were obtained by confocal microscopy (Nikon)

Cytotoxicity. MCF-7 cells were plated onto 96-well plates. The cells were incubated with peptides for 24 h. Then, 10 μL of Cell Counting Kit-8 solution was added and incubated for 1 h. After incubation, the absorbance of plates at 450 nm was measured on a Multiskan FC microplate reader (Thermo Scientific).

Docking Simulation. Docking studies of peptides **5** and **17** and the VDR (PDB: 5H1E)[14] were performed using Molecular Operating Environment (MOE) 2020.0901. Before the docking studies, a conformation search of peptides was performed. During the simulation, the distances and angles between the atoms that were presumed to form hydrogen bonds in the backbone were constrained (1.6–3.0 Å, 160–180°) based on the results of the secondary structure analysis. The binding site of the protein was defined as the LXXLL motif in the X-ray structure. The docking simulations of peptides bound to the VDR were carried out using standard protocols of general docking. All docking poses were first ranked by the London dG score, then a force field refinement was performed on the top 400 poses, followed by rescoring of GBVI/WSA dG. The force field used for calculating the conformations was the Amber10:EHT[37] force field.

Real-Time PCR. Real-time PCR was performed as previously reported.[38] Briefly, after HL-60 cells were treated with VD$_3$ with or without peptides for 48 h, total RNA was isolated using the TRIzol reagent (Thermo, Waltham, MA), according to the manufacturer's instructions. qPCR assays were conducted using a QuantiTect SYBR Green RT-PCR Kit (QIAGEN, Valencia, CA) and a ViiA7 real-time PCR system (Applied Biosystems, Foster City, CA). The relative changes in transcript levels for each sample were determined by normalization to the GAPDH mRNA levels. The following primers were used for real-time PCR: p21, forward, 5′-AAGACCATGTGGACCTGTCACTGT-3′ and reverse, 5′-GAAGATCAGCCGGCGTTTG-3′ GAPDH, forward, 5′-GTCTCCTCTGACTTCAACAGCG-3′ and reverse, 5′-AC-CACCCTGTTGCTGTAGCCAA-3′.

NBT Reduction Assay. The NBT reduction assay was performed as previously reported.[39] Briefly, after HL-60 cells were treated with VD$_3$ with or without peptides for 48 h, the cells were stained with 1 mg/mL NBT (WAKO, Osaka, Japan) and 320 nM Phorbol 12-myristate 13-acetate (Sigma-Aldrich, St. Louis, MO) for 30 min at 37 °C. NBT-positive and -negative cells were microscopically counted from more than 200 cells, and the percentage of NBT-positive cells was calculated.

■ ASSOCIATED CONTENT

⑤ **Supporting Information**

The Supporting Information is available free of charge at https://pubs.acs.org/doi/10.1021/acsomega.2c05409.

> Results of CD spectra analysis; enzyme resistance assay; flow cytometry; CLSM observation; cytotoxicity assay; and HPLC analysis of peptides (PDF)

■ AUTHOR INFORMATION

Corresponding Authors

Takashi Misawa − *National Institute of Health Sciences, Kawasaki, Kanagawa 210-9501, Japan;* ⑩ orcid.org/0000-0002-0339-8750; Phone: +81-44-270-6580; Email: Misawa@nihs.go.jp; Fax: +81-44-270-6578

Yosuke Demizu − *National Institute of Health Sciences, Kawasaki, Kanagawa 210-9501, Japan; Graduate School of Medical Life Science, Yokohama City University, Yokohama, Kanagawa 230-0045, Japan; Graduate School of Medicine, Dentistry and Pharmaceutical Sciences, Okayama University, Kita-ku, Okayama 700-8530, Japan;* ⑩ orcid.org/0000-0001-7521-4861; Phone: +81-44-270-6578; Email: demizu@nihs.go.jp; Fax: +81-44-270-6578

Authors

Mami Takyo − *National Institute of Health Sciences, Kawasaki, Kanagawa 210-9501, Japan; Graduate School of Medical Life Science, Yokohama City University, Yokohama, Kanagawa 230-0045, Japan*

Yumi Sato − *National Institute of Health Sciences, Kawasaki, Kanagawa 210-9501, Japan; Graduate School of Medical Life Science, Yokohama City University, Yokohama, Kanagawa 230-0045, Japan*

Naoya Hirata − *National Institute of Health Sciences, Kawasaki, Kanagawa 210-9501, Japan*

Keisuke Tsuchiya − *National Institute of Health Sciences, Kawasaki, Kanagawa 210-9501, Japan; Graduate School of Pharmacy, Showa University, Shinagawa-ku, Tokyo 142-8555, Japan*

Hiroaki Ishida − *Laboratory of Drug Design and Medicinal Chemistry, Showa Pharmaceutical University, Machidashi, Tokyo 194-8543, Japan;* orcid.org/0000-0003-0341-2660

Takashi Kurohara − *National Institute of Health Sciences, Kawasaki, Kanagawa 210-9501, Japan;* orcid.org/0000-0003-4228-3478

Yuta Yanase − *National Institute of Health Sciences, Kawasaki, Kanagawa 210-9501, Japan; Graduate School of Medical Life Science, Yokohama City University, Yokohama, Kanagawa 230-0045, Japan*

Takahito Ito − *National Institute of Health Sciences, Kawasaki, Kanagawa 210-9501, Japan; Graduate School of Medical Life Science, Yokohama City University, Yokohama, Kanagawa 230-0045, Japan*

Yasunari Kanda − *National Institute of Health Sciences, Kawasaki, Kanagawa 210-9501, Japan*

Keiko Yamamoto − *Laboratory of Drug Design and Medicinal Chemistry, Showa Pharmaceutical University, Machidashi, Tokyo 194-8543, Japan;* orcid.org/0000-0001-6642-7961

Complete contact information is available at:
https://pubs.acs.org/10.1021/acsomega.2c05409

Author Contributions

T.M. and Y.D. designed the research and wrote the paper. M.T., Y.S., N.H., K.T., H.I., T.K., and T.I. performed the experiments and analyzed the results. All authors discussed the results and commented on the manuscript.

Notes

The authors declare no competing financial interest.

REFERENCES

(1) Jones, G.; Strugnell, S. A.; Dluca, H. F. Current understanding of the molecular actions of vitamin D. *Physiol. Rev.* **1998**, *78*, 1193−1231.

(2) Roodman, G. D.; Windle, J. J. Paget disease of bone. *J. Clin. Invest.* **2005**, *115*, 200−208.

(3) Ozono, K.; Saito, M.; Miura, D.; Michigami, T.; Nakajima, S.; Ishizuka, S. Analysis of the molecular mechanism for the antagonistic action of a novel 1α,25-dihydroxyvitamin D3 analogue toward vitamin D receptor function. *J. Biol. Chem.* **1999**, *274*, 16392−16399.

(4) Herdick, M.; Steinmeyer, A.; Carlberg, C. Antagonistic action of a 25-carboxylic ester analogue of 1α,25-dihydroxyvitamin D3 is mediated by a lack of ligand-induced vitamin D receptor interaction with coactivator. *J. Biol. Chem.* **2000**, *275*, 16506−16512.

(5) Nakano, Y.; Kato, Y.; Imai, K.; Ochiai, E.; Namekawa, J.; Ishizuka, S.; Takenouchi, K.; Tanatani, A.; Hashimoto, Y.; Nagasawa, K. Practical synthesis and evaluation of the biological activities of 1α,25-dihydroxyvitamin D3 antagonists, 1α,25-dihydroxyvitamin D3-26,23-lactams. Designed on the basis of the helix 12-folding inhibition hypothesis. *J. Med. Chem.* **2006**, *49*, 2398−2406.

(6) Belorusova, A. Y.; Chalhoub, S.; Rovito, D.; Rochel, N. Structural analysis of VDR complex with ZK168281 antagonist. *J. Med. Chem.* **2020**, *63*, 9457−9463.

(7) Sakamaki, Y.; Inaba, Y.; Yoshimoto, N.; Yamamoto, K. Potent Antagonist for the Vitamin D Receptor: Vitamin D Analogues with Simple Side Chain Structure. *J. Med. Chem.* **2010**, *53*, 5813−5826.

(8) Kato, A.; Anami, Y.; Egawa, D.; Itoh, T.; Yamamoto, K. Helix12-stabilization antagonist of vitamin D receptor. *Bioconjugate Chem.* **2016**, *27*, 1750−1761.

(9) Kato, A.; Yamao, M.; Hashihara, Y.; Ishida, H.; Itoh, T.; Yamamoto, K. Vitamin D analogues with a p-hydroxyphenyl group at the C25 position: crystal structure of vitamin D receptor ligand-binding domain complexed with the ligand explains the mechanism underlying full antagonistic action. *J. Med. Chem.* **2017**, *60*, 8394−8406.

(10) Teska, K. A.; Bogart, J. W.; Arnold, A. A. Novel VDR antagonists based on the GW7042 scaffold. *Bioorg. Med. Chem. Lett.* **2018**, *28*, 351−354.

(11) Heery, D. M.; Kalkhoven, E.; Hoare, S.; Parker, M. G. A signature motif in transcriptional co-activators mediated binding to nuclear receptors. *Nature* **1997**, *387*, 733−736.

(12) Kim, S.; Shevde, N. K.; Pike, J. W. 1α,25-Dihydroxyvitamin D3 stimulates cyclic vitamin D receptor/retinoid receptor DNA binding, co-activator recruitment, and histone acetylation in intact ostepblasts. *J. Bone Miner. Res.* **2005**, *20*, 305−317.

(13) Mita, Y.; Dodo, K.; Noguchi-Yachide, T.; Hashimoto, Y.; Ishikawa, M. Structure-activity relationship of benzodiazepine derivatives as LXXLL peptide mimetics that inhibit the interaction of vitamin receptor with coactiators. *Bioorg. Med. Chem.* **2013**, *21*, 993−1005.

(14) Egawa, D.; Itoh, T.; Kato, A.; Kataoka, S.; Anami, Y.; Yamamoto, K. SRC2-3 binds to vitamin D receptor with high sensitivity and strong affinity. *Bioorg. Med. Chem.* **2017**, *25*, 568−574.

(15) Cussol, L.; Mauran-Ambrosino, L.; Buratto, J.; Belorusova, A. Y.; Neuvila, M.; Osz, J.; Furibourg, S.; Fremaux, J.; Dolan, C.; Goudreau, S. R.; Rochel, N.; Guichard, G. Structural basis for α-helix mimicry and inhibition of protein-protein interaction with oligourea foldamers. *Angew. Chem., Int. Ed.* **2021**, *60*, 2296−2303.

(16) Ran, X.; Gestwicki, J. E. Inhibition of Protein−protein interactions (PPIs): An analysis of scaffold choices and buried surface area. *Curr. Opin. Chem. Biol.* **2018**, *44*, 75−86.

(17) Marqus, S.; Pirogova, E.; Piva, T. J. Evaluation of the use of therapeutic peptides for cancer treatment. *J. Biomed. Sci.* **2017**, *24*, 21.

(18) Harms, M.; Hansson, R. F.; Carmali, S.; Almeida-harández, Y.; Sanchez-Garcia, E.; Münch, J.; Zelikin, A. N. Dimerization of the peptide CXCR4-antagonist on macromolecular and supramolecular protraction affords increased potency and enhanced plasma stability. *Bioconjugate Chem.* **2022**, *33*, 594−607.

(19) Zhu, Q.; Chen, Z.; Paul, P. K.; Lu, Y.; Wu, W.; Qi, J. Oral delivery of proteins and peptides: challenges, status quo and future perspectives. *Acta Pharm. Sin. B* **2021**, *11*, 2416−2448.

(20) Johnson, L. M.; Mortenson, D. E.; Yun, H. G.; Horne, W. S.; Ketas, T. J.; Lu, M.; Moore, J. P.; Gellman, S. H. Enhancement of α-helix mimicry by an α/β-peptide foldamer via incorporation of a dense Ionic side-chain array. *J. Am. Chem. Soc.* **2012**, *134*, 7317−7320.

(21) Bindl, D.; Mandal, P. K.; Huc, I. Generalizing the aromatic δ-amino acid foldamer helix. *Chem. - Eur. J.* **2022**, *28*, No. e202200538.

(22) Kim, Y. W.; Grossmann, T. N.; Verdine, G. L. Synthesis of all-hydrocarbon stapled α-helical peptides by ring-closing olefin meta-thesis. *Nat. Protoc.* **2011**, *6*, 761−771.

(23) Hirano, M.; Saito, C.; Goto, C.; Yokoo, H.; Kawano, R.; Misawa, T.; Demizu, Y. Rational design of helix-stabilized antimicrobial peptide foldamers containing α,α-disubstituted amino acids or side-chain stapling. *ChemPlusChem* **2020**, *85*, 2731−2736.

(24) Gellman, S. H. Foldamers: A Manifest. *Acc. Chem. Res.* **1998**, *31*, 173−180.

(25) Cebrele, C.; Martinek, T. A.; Reiser, O.; Berlicki, Ł. Peptide containing β-amino acid patterns: challenges and successes in medicinal chemistry. *J. Med. Chem.* **2014**, *57*, 9718−9739.

(26) Misawa, T.; Ohoka, N.; Oba, M.; Yamashita, H.; Tanaka, M.; Naito, M.; Demizu, Y. Development of 2-aminoisobutyric acid (Aib)-rich cell-penetrating foldamers for efficient siRNA delivery. *Chem. Commun.* **2019**, *55*, 7792−7795.

(27) Misawa, T.; Demizu, Y.; Kawamura, M.; Yamagata, N.; Kurihara, M. Structural development of stapled short helical peptides as vitamin D receptor (VDR)-coactivator interaction inhibitors. *Bioorg. Med. Chem.* **2015**, *23*, 1055−1061.

(28) Nagakubo, T.; Demizu, Y.; Kanda, K.; Misawa, T.; Shoda, T.; Okuhira, K.; Sekino, Y.; Naito, M.; Kurihara, M. Development of cell-penetrating R7 fragment-conjugated helical peptides as inhibitors of estrogen receptor-mediated transcription. *Bioconjugate Chem.* **2014**, *25*, 1921−1924.

(29) Boersma, M. D.; Haase, H. S.; Kaufman, K. J. P.; Lee, E. F.; Clarke, O. B.; Colman, P. M.; Smith, B. J.; Horne, W. S.; Fairlie, W. D.; Gellman, S. H. Evaluation of diverse α/β-backbone patterns for functional α-helix mimicry: analogues of the Bim BH3 domain. *J. Am. Chem. Soc.* **2012**, *134*, 315−323.

(30) Suzuki, T.; Futaki, S.; Niwa, M.; Tanaka, S.; Ueda, K.; Sugiura, Y. Possible existence of common intermnalization mechanisms among arginine-rich peptides. *J. Biol. Chem.* **2002**, *277*, 2437−2443.

(31) Rothbard, J. B.; Jessop, T.; Lewis, R. S.; Murray, B. A.; Wender, P. A. Role of membrane potential and hydrogen bonding in the mechanis of translocation of guanidinium-rich peptides into cells. *J. Am. Chem. Soc.* **2004**, *126*, 9506−9507.

(32) Schmitt, M. A.; Weisblum, B.; Gellman, S. H. Interplay among folding, sequence, and lipophilicity in the antibacterial and hemolytic activities of α/β-peptides. *J. Am. Chem. Soc.* **2007**, *129*, 417−428.

(33) Masuno, H.; Ikura, T.; Morizono, D.; Orita, I.; Yamada, S.; Shimizu, M.; Ito, N. Crystal structure of complexes of Vitamin D

receptor ligand-binding domain with litocholic acid derivatives. *J. Lipid Res.* **2013**, *54*, 2206−2213.

(34) Sato, H.; Felix, J. B. Peptide-membrane interaction and mechanisms of membrane destruction by amphipathic a-helical antimicrobial peptides. *Biochim. Biophys. Acta, Biomembr.* **2006**, *1758*, 1245−1256.

(35) Liu, M.; Lee, M.; Cohen, M.; Bommakanti, M.; Freedman, L. P. Transcriptional activation of the Cdk inhibitor p21 by vitamin D3 leads to the induced differentiation of the myelomonocytic cell line U937. *Genes Dev.* **1996**, *10*, 142−153.

(36) De Araujo, A. D.; Lim, J.; Wu, K. C.; Hoang, H. N.; Nguyen, H. T.; Fairlie, D. P. Landscaping macrocyclic peptides: stapling hDM2-binding peptides for helicity, protein affinity, proteolytic stability and cell uptake. *RSC Chem. Biol.* **2022**, *2*, 895−904.

(37) Case, D. A.; Darden, T. A.; Cheatham, T. E.; Simmerling, C. L.; Wang, J.; Duke, R. E.; Luo, R.; Crowley, M.; Walker, R. C.; Zhang, W.; Merz, K. M.; Wang, B.; Hayik, S.; Roitberg, A.; Seabra, G.; Kolossváry, I.; Wong, K. F.; Paesani, F.; Vanicek, J.; Wu, X.; Brozell, S. R.; Steinbrecher, T.; Gohlke, H.; Yang, L.; Tan, C.; Mongan, J.; Hornak, V.; Cui, G.; Mathews, D. H.; Seetin, M. G.; Sagui, C.; Babin, V.; Kollman, P. A. *AMBER 10*; University of California: San Francisco, 2008.

(38) Tsuji, K.; Yamada, S.; Hirai, K.; Asakura, H.; Kanda, Y. Development of alveolar and airway cells from human iPS cells: toward SARS-CoV-2 research and drug toxicity testing. *J. Toxicol. Sci.* **2021**, *46*, 425−435.

(39) Sasaki, H.; Masuno, H.; Kawasaki, H.; Yoshihara, A.; Numoto, N.; Ito, N.; Ishida, H.; Yamamoto, K.; Hirata, N.; Kanda, Y.; Kawachi, E.; Kagechika, H.; Tanatani, A. Litocholic acid derivatives as potent vitamin D receptor agonists. *J. Med. Chem.* **2021**, *64*, 516−526.